Increased hydrostatic pressure enhances motility of lung cancer cells

Yu-Chiu Kao, Chau-Hwang Lee and Po-Ling Kuo*

Abstract—**Interstitial fluid pressures within most solid tumors are significantly higher than that in the surrounding normal tissues. Therefore, cancer cells must proliferate and migrate under the influence of elevated hydrostatic pressure while a tumor grows. In this study, we developed a pressurized cell culture device and investigated the influence of hydrostatic pressure on the migration speeds of lung cancer cells (CL1-5 and A549). The migration speeds of lung cancer cells were increased by 50–60% under a 20 mmHg hydrostatic pressure. We also observed that the expressions of aquaporin in CL1-5 and A549 cells were increased under the hydrostatic pressure. Our preliminary results indicate that increased hydrostatic pressure plays an important role in tumor metastasis.**

I. INTRODUCTION

High interstitial fluid pressure (IFP) is a hallmark of many advanced cancers. The increase of IFP may result from high vessel permeability, low lymphatic drainage, poor perfusion, and high cell density around the blood vessels. For example, the IFP was reported to increase to 29 mmHg in breast carcinoma and 34 mmHg in osteosarcoma. A high IFP usually impedes the therapeutic effects of anticancer drugs or macromolecules by reducing the delivery and uptake of the chemicals.[1-4]

There is a growing body of evidence suggesting that the increased IFP plays a role in promoting the motility and invasiveness of cancer cells.[5-8] Cell migration is a highly orchestrated process in which cell movements are guided by both internal signals and signals from the microenvironment. Interstitial flow driven by the difference of IFP between different parts of a tumor generates cytokine gradients and alter stromal cell behavior in the tumor microenvironment. However, how the motility of cancer cells is affected by fluid pressure increased up to 10—40 mmHg has been barely addressed.

We hypothesized that high fluid pressure enhances motility of cancer cells by up regulating aquaporin, a transmembrane water channel protein that modulates the water content of a cell. Aquaporins (AQPs) are water-permeable proteins found in cell membranes of prokaryotes and various mammalian tissues. The increased fluid pressure may accelerate water transport through cancer cells, facilitate change of cellular morphology, and consequently promote cell migration. Aquaporin has been found to play a critical role in cell migration and migration-associated cell function such as angiogenesis, wound healing, and neutrophil motility.[9]

In this regard, we investigated the effects of high fluid pressure on the motility and aquaporin activities of lung cancer cells. We developed a microfluidic device that allows to exert fluid pressure ranging from 0 to 60 mmHg on cultured cells. Time lapsed images were taken to track the migration of individual cells. The changes of cellular morphology and water content when cells were subject to high fluid pressure were determined by a recently developed technique called digital holographic microtomography, which generates a three-dimensional map of refractive index inside a cell. In general, the mean refractive index of a cell is higher than that of water; a decrease of the mean values indicates water inflow and vice versa. Quantitative immunocytochemistry was employed to determine the amount of specific proteins, including aquaporin, vinculin, and rac1, in cells subject to high fluid pressure.

II. MATERIALS AND METHODS

A. Chip fabrication

The layout and pressure characteristics of the cell culture chip used in the present work is shown in Figure 1. The chip was mainly made of polydimethylsiloxane (PDMS), a biocompatible, transparent material suitable for live cell imaging with optical microscopy in the visible spectral regime. It is also simpler in shaping and assembly of the chip using PDMS when compared with other plastics. The cell culturing chamber was disc-like with a radius of 6 mm and a height of 70 μm (Figure 1a). The PDMS replicas were made by casting PDMS over PMMA masters and then bonded on a glass slide after treated with oxygen plasma.

To study the effects of hydrostatic pressures on the migration of cancer cells, we pressurized the cell culturing chamber using a syringe pump (NE-1000, New Era Pump Systems, USA). A pressure gauge (700G04, Fluke, USA) was connected to the outlet of the chamber to measure the temporal profile of fluid pressure. As shown in Figure 1b, the fluid pressure in the cell culturing chamber increased almost linearly when extra fluid was added into the chamber. However, since PDMS is a viscoelastic material, the pressure dropped gradually as time passed due to the so-called "stress-relaxation" phenomenon (Figure 1c). Nevertheless, we found that the pressure inside the chamber can be kept stable as long as the chamber was perfused at constant rates of flow, which were around 1.6~1.8 μl/min.

* Research supported by the Ministry of Economic Affairs of Taiwan with grant number 102-EC-17-A-19-S1-174.

Yu-Chiu Kao is with Graduate Institute of Biomedical Electronics and Bioinformatics, National Taiwan University, Taipei, Taiwan, (winifred@gate.sinica.edu.tw)

Chau-Hwang Lee is with Research Center for Applied Sciences, Academia Sinica, Taiwan, (clee@gate.sinica.edu.tw)

Po-Ling Kuo is with Graduate Institute of Biomedical Electronics and Bioinformatics and department of Electrical Engineering, National Taiwan University, Taipei, Taiwan (corresponding author; phone: +886-3366-9882; e-mail: poling@ntu.edu.tw).

B. Cell culture

Human lung adenocarcinomic cells A549 were cultured in a Kaighn's modified Ham's F-12K Medium (21127, Gibco, Life Technologies, Taipei, Taiwan) with 10% fetal bovine serum and 1% antibiotic pen-strep-amphotericin. Human lung adenocarcinoma cells CL1-5 were cultured with Dulbecco's Modified Eagle's Medium (DMEM) (11965, Gibco, Life Technologies, Taipei, Taiwan) supplemented with 10% fetal bovine serum and 1% antibiotic pen-strep-amphotericin.

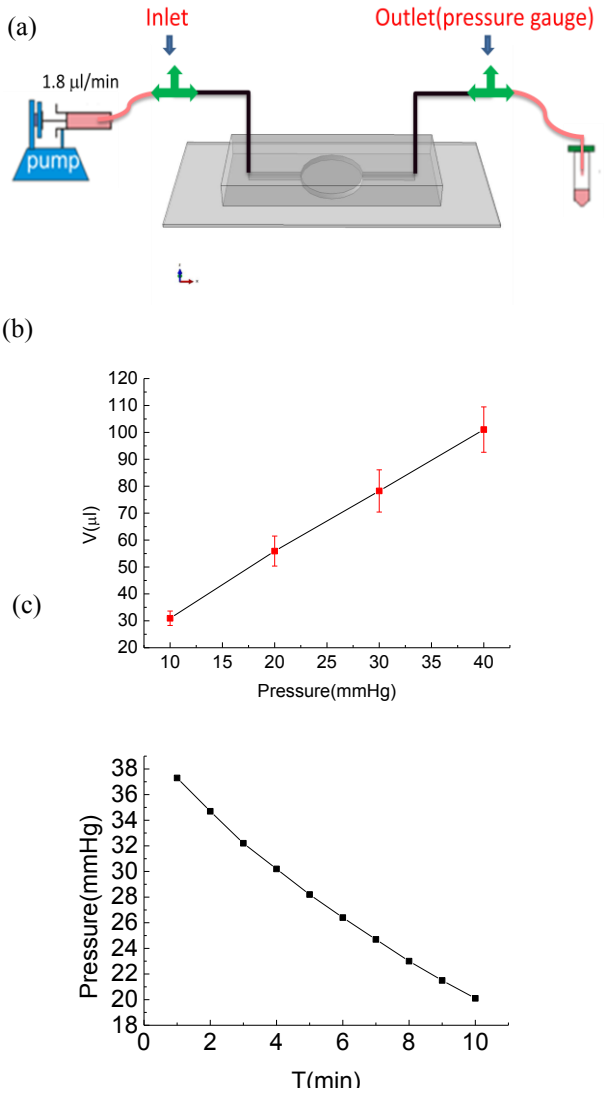

FIG. 1. (a) Schematic of the cell culturing chip. (b) Characteristics of the chip pressures. (c) Stress relaxation in the PDMS chip.

C. Digital holographic microtomography

The details of the working principle and setup of the digital holographic microtomography (DHmT) system have been described previously.[10] In brief, the DHmT system is based on a Mach-Zehnder heterodyne interferometer in which phase shifting of the reference beam relative to the sample beam is generated by a mirror mounted on an openloop PZT (AE0505D16, NEC, Taiwan). A 405 nm diode laser (Ming Home Photonics, Taiwan) was employed as light source. A polarization beam splitter (Singapore Optics Shop, Signgapore) was used to divide the laser beam into s-wave and p-wave which are referred to as reference beam and sample beam, respectively. A half-wave plate (Lambda Research Optics, Inc., Costa Mesa , CA, USA), WP1, wass used to adjust light intensities of these two beams. Another half-wave plate (Lambda Research Optics, Inc.),WP2, rotated polarization of the reference beam to p-wave to interfere with the sample beam after the reference and sample beams were recombined by a non-polarization beam splitter (Singapore Optics Shop), NPBS. The sample beam wass focused by a scan lens (f =75 mm) to the back focal plane of an oilimmersion 100x objective lens, OL1, to generate planar wave illumination. Different illumination angles are achieved by a galvanometer scanning mirror (Nutfield Technology, Inc., Hudson, NH, USA), SM. Another oil-immersion 100x objective lens, OL2, collects transmitted illumination light and scattered light which were projected onto a highspeed CMOS camera (VDS Vosskühler GmbH, Osnabrück, Germany) by a tube lens (f = 250 mm) to form interference images. This camera captures 485 frames per second. Data acquisition was performed using a home-made Windows application software written in C++. To estimate the change of cell volume after application of hydrostatic pressure, the cells were fixd using a a solution of 4% paraformaldehyde (Electron Microscopy Sciences, Hatfield,PA, USA) in PBS at room temperature, and imaged using the DHmT. Two-dimensional phase images of the cells were extracted from multiple interference images with various phase shifts between the reference and the sample beams. The phase at a location was proportional to the line integral of refractive index along the path of the light ray passing through the location. In analogy to X-ray computed tomography, phase images obtained at various incident angles were used to reconstruct 3D refractive index distribution of the cells based on the theory of optical diffraction tomography. This yielded a set of 2D image slices across the height of the cells at an increment of 1 μm. Since the refractive index of cells is usaully larger than that of water, the region inside a cell on individual slices can be easily differentiated from that outside of the cell as long as the cell is surrounded by water. Thus the volume of the cell transected by a particular image slice was estimated to be the product of the cellular area and the slice thickness (i.e., 1 μm). Summing up the volumes across the image set gave the total volume of the cells.

D. Cell tracking

Live cell images were acquired every 10 minute using a 10×, NA 0.25 objective installed on Olympus IX71 inverted microscope (Olympus Australia, Mt. Waverley, Australia). A LABVIEW-based program was employed to identify the boundary of a cell on a DIC image and to determine the centroid of the cell using the definition

$$x_c = \Sigma_{i=1}^{m} x_i / m, \quad y_c = \Sigma_{i=1}^{m} y_i / m, \qquad (1)$$

where (x_i, y_i) and m represent the coordinates and number of

the individual pixels within the boundary of the cell respectively. The migration speeds of individual cells were calculated by dividing the distance between the cell centroids measured from two consecutive images by the sampling interval. The cells were tacked for 8 hrs. The tracking expriments were conducted at least three times for each cell types and more than 15 cells were tracked in individual experiments.

E. Quantitative immunocytochemistry

To determine the relation between hydrostatic pressue and AQPs, we exposed the A549 and CL1-5 cells to hydrostatic pressures varying from 0 to 20 mmHg for 8 hrs. Afterwards the cells were fixed with a solution of 4% paraformaldehyde in PBS, and blocked with 1% BSA for 1 hr at room temperature. The fixed cells were incubated with primary antibodies (1:500 rabbit AQP-1 antibody in blocking solution; Gene Tex Inc., Irvine,CA, USA) overnight at 4°C, as described previously [11], and incubated with fluorophore conjugated secondary antibodies (1:400 Alexa Fluor 488 goat antirabbit in blocking solution; A-11008, Life Technologies, USA) for 2 hr at room temperature. The fluorescence intensity of individual cells were quantified using the ImageJ (http://rsb.info.nih.gov/ij/).

III. RESULTS AND DISCUSSION

A. Hydrostatic pressure increases speeds of cell migration

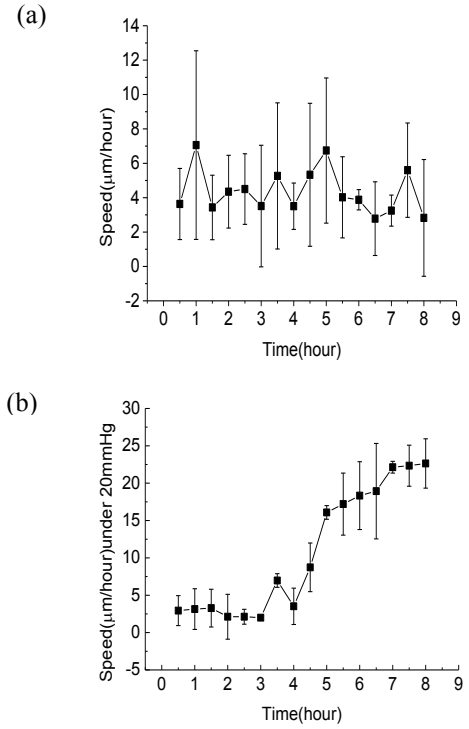

FIG.2. Temporal profiles of migration speed of A549 cells that were (a) not pressurized (n=14) and (b) pressurized (n=11) with hydrostatic pressure of 20 mmHg for 8 hrs. The data were averaged from 25 and 17 cells in (a) and (b), with that the error bars represent

The typical temporal patterns of the migration speeds of A549 cells exposed to hydrostatic pressure of 0 and 20 mmHg are shown in Figure 2. The migration speeds of the cells not pressurized did not vary significantly with time, while the speeds of the pressurized cells appear to increase after pressure exposure of 4 hr and the effects of pressure on migration speed lasted to the end of the expriment. Similar results were found in other cells.

Since the effect of hydrostatic pressure on cell migration is more prominent after 4 hour of pressure treatment, we focused the cell tracking on the data recorded at five to eight hours of pressurization. Figure 3 summarized the effects of applying various hydrostatic pressures on the migration speeds of the A549 and CL1-5 cancer cells. The migration speeds of both types of cell increased significantly with increasing hydrostatic pressures. In particular when exposed to hydrostatic pressure of 20 mmHg, the A549 cell moved about three times faster than that without pressure application.

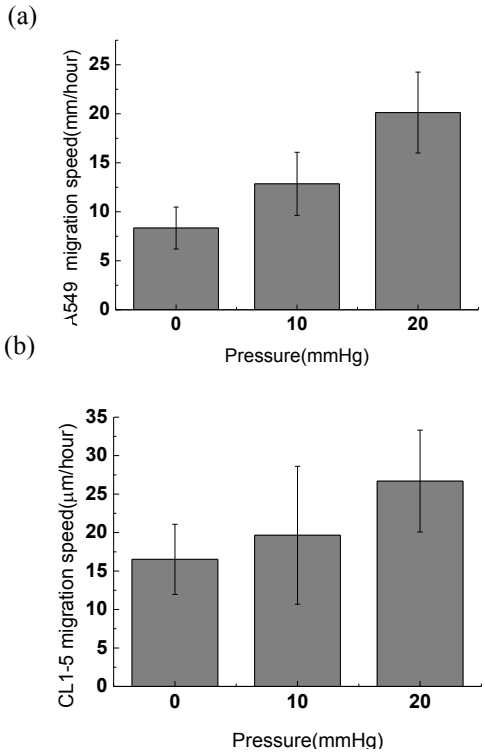

FIG.3. The mean and standard deviations of the migration speeds of (a) A549 and (b) CL1-5 cells exposed to various hydrostatic pressures.

B. Cell deformation induced by hydrostatic pressure

We wondered whether the application of hydrostatic pressure significantly changes cell morphology by driving water influx/outlfux of the cells. To dermine this, we calcualted the change of cell volume and intracellular refractive index (RI) when exposed to hydrostatic pressures varying from 0 to 10 mmHg for 8 hrs using a newly

developed imaging technique called DHmT. As shown in Figure 4, the application of hydrostatic pressure of 10 mmHg increased the cell volume about 2 times when compared with that withoout pressurizaton.

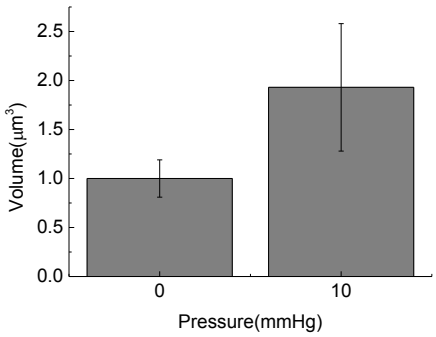

FIG.4. The mean and standard deviations of the cell volumes of CL1-5 cells exposed to various hydrostatic pressures (n=9).

C. Hydrostatic pressure enhanced AQP-1 expression

Quantitative immunocytochemistry revealed that the expression of AQP-1 increased with the increasing hydrostatic pressures in both CL1-5 and A549 cells , as shown in Figure 5. These findings support the data presented in Figure 3 and 4 and imply that the increased migration speeds and the increased cell volumes in lung cancer cells after exposure of hydrostatic pressure may at least in part result from the increased activities of AQP-1.

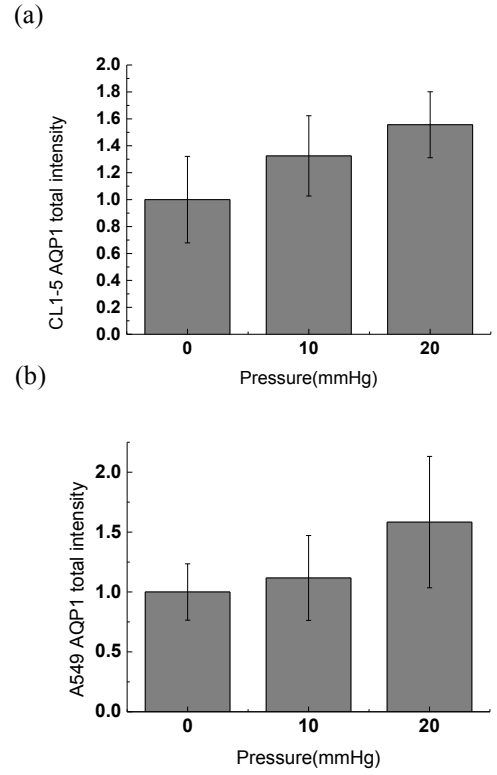

Fig5. Relations between applied pressures and AQP activities in (a) CL1-5 and (b) A549 cells.

IV. CONCLUSION

In the present work, we built a microfluidic device to study the effects of increased hydrostatic pressures on the mechanobiology of cells. Our preliminary results suggest that increased hydrostatic pressure increases the migration speeds and cell volume of lung cancer cells, and such effects may result from the increased activities of aquaporin-1.

.

References

[1] D. T. Butcher, T. Alliston, and V. M. Weaver, "A tense situation: forcing tumour progression," *NATURE,* vol. 9, 2009.

[2] S. Ferretti, P. R. Allegrini, M. M. Becquet, and P. M. J. McSheehy, "Tumor Interstitial Fluid Pressure as an Early-Response Marker for Anticancer Therapeutics," *neoplasia,* vol. 11, 2009.

[3] M. Hofmann, M. Guschel, A. Bernd, J. r. Bereiter-Hahny, R. Kaufmann, C. Tandiz, H. Wiig, and S. Kippenberger, "Lowering of Tumor Interstitial Fluid Pressure Reduces Tumor Cell Proliferation in a Xenograft Tumor Model1," *Neoplasia,* vol. 8, 2006.

[4] P. A. Torzilli, J. W. Bourne, T. Cigler, and C. T. Vincent, "A new paradigm for mechanobiological mechanisms in tumor metastasis," *Seminars in Cancer Biology,* vol. 22, 2012.

[5] A. C. Shieh and M. A. Swartz, "Regulation of tumor invasion by interstitial fluid flow," *PHYSICAL BIOLOGY,* vol. 8, 2011.

[6] T. G. Simonsen, J.-V. Gaustad, M. N. Leinaas, and E. K. Rofstad, "High Interstitial Fluid Pressure Is Associated with Tumor-Line Specific Vascular Abnormalities in Human Melanoma Xenografts," *PLoS ONE,* vol. 7, 2012.

[7] T. Stylianopoulos, J. D. Martin, M. Snuderl, F. Mpekris, S. R.Jain, and R. K. Jain, "Co-evolution of solid stress and interstitial fluid pressure in tumors during progression: Implications for vascular collapse," *Cancer Research,* vol. 10, p. 3833, 2013.

[8] J. Tien, J. G., and T. C. M. Nelson, "Modulation of Invasive Phenotype by Interstitial Pressure-Driven Convection in Aggregates of Human Breast Cancer Cells," vol. 7, 2012.

[9] Y. Jiang, "Aquaporin-1 Activity of Plasma Membrane Affects HT20 Colon Cancer Cell Migration," *IUBMB Life,* vol. 61, 2009.

[10] J.-W. Su, W.-C. Hsu, C.-Y. Chou, C.-H. Chang, and K.-B. Sung, "Digital holographic microtomography for high-resolution refractive index mapping of live cells," *Biophotonics,* vol. 6, 2013.

[11] M. B. Arciszewski, M. Stefaniak, A. Zacharko-Siembida, and J. Całka, "Aquaporin 1 water channel is expressed on submucosal but not myenteric neurons from the ovine duodenum," *Annals of Anatomy,* vol. 193, 2011.